Torque Ripple Minimization for Direct Torque Control of PMSM With Modified FCSMPC

Qian Liu and Kay Hameyer, *Senior Member, IEEE*

***Abstract*—In this paper, a Lyaupnov-based finite control set model predictive direct torque control for the permanent magnet synchronous machine (PMSM) is proposed. In the proposed control scheme, the finite control set prediction and the Lyapunov theory are combined to minimize the torque ripple. The eight voltage vectors of the two-level converter are utilized as a finite control set for the torque prediction of the PMSM. A cost function considering the torque error, the maximum torque per ampere operation and the current limitation is introduced. Comparing to the conventional finite control set predictive control, the dominant part of the cost function is utilized as a Lyapunov function to estimate the duty cycle of each voltage vector. An optimum voltage can be obtained by the optimum voltage vector from the eight vectors and their duty cycles. A small sampling frequency and a fixed switching frequency can be realized when compared to the conventional finite set model predictive control. In the end, the simulation and experimental results validate the performance of the proposed control scheme.**

***Index Terms*—Current ripple, direct torque control (DTC), finite control set MPC (FCSMPC), fixed switching frequency, Lyapunov-based duty cycle, maximum torque per ampere (MTPA), permanent magnet synchronous machine (PMSM), torque ripple.**

I. Introduction

NOWDAYS, the permanent magnet synchronous machine (PMSM) is very popular in the electrical drive system in the industry due to its large torque density and high efficiency. In order to achieve a fast torque response for the PMSM, the direct torque control (DTC) is introduced as an alternative of the field oriented control (FOC). Compared to the FOC, the torque response with DTC is much faster since it is without the current control loop [1]–[3]. The conventional DTC is realized by two nonlinear hysteresis comparators and a switching table of the converter status [2], [4], [5]. Each of the selected converter status lasts for one sampling period of the digital controller, which results in variable switching frequency and large current and torque ripples.

In order to reduce the torque and current ripples, a revised DTC has been proposed to be combined with the space vector pulse width modulation (SVPWM) [6], [7]. A PI torque controller is introduced to calculate the voltage reference, which is implemented by the SVPWM. Therefore, the continuous voltage and constant switching frequency of the converter can be realized to reduce the current and torque ripple. However, the torque response varies depending on the gain of the PI controller [7], [8], which degrades the advantages of the DTC when compared to the FOC.

Currently, along with the development of the predictive control, numerous methods, such as the torque predictive control (TPC) and the model predictive control (MPC) are proposed for the torque control to achieve high performance for the PMSM. The TPC calculates the reference stator voltage for the desired torque and flux according to the torque and voltage equation of the PMSM in a predictive way [8]–[10]. The switching frequency of the converter is constant, since the TPC is combined with the SVPWM. The torque ripple can be reduced by the TPC, if a variable duty cycle of the reference stator voltage is introduced. The duty cycle can be calculated in such a way that the mean torque error equals to zero in one sampling period. However, the TPC is inconvenient to consider the system constraints such as the limitation of the current and a certain level of the torque ripple remains. In order to improve both torque ripples and torque response for the PMSM, a specific DTC named as Deadbeat DTC is proposed [11]–[13]. Optimization of losses and response time can be considered in the Deadbeat DTC. However, the algorithm is relatively complicated.

For the model predictive DTC, a finite set of the natural voltage vectors of the inverter [(e.g., eight voltage vectors for the two-level inverter] is utilized as a search table to optimize the predefined cost function. One major advantage for the finite control set MPC (FCSMPC) is that a general form for the cost function can be introduced to optimize the system performance considering different system constraints [14], [15]. Therefore, a cost function considering the torque response for the PMSM can be utilized to realize the DTC [16]–[18] and special objectives such as the maximum torque per ampere (MTPA) condition can be taken into account [19]. However, the torque control using conventional FCSMPC has the same disadvantages as the conventional DTC. Each converter status lasts for one sampling period, which results in large torque and current ripples and degrades the performance of the PMSM. In [20], a torque ripple compensation is applied to the PMSM with FCSMPC for reduction of the cogging torque. However, the torque ripples caused by the switching of the inverter are not reduced. In order to reduce the current and torque ripples for the FCSMPC, several modifications such as quantized searching [21] and a duty cycle control [22]–[24]. With both modifications, the torque and current ripples can be reduced.

Manuscript received March 30, 2016; revised May 27, 2016 and June 17, 2016; accepted August 8, 2016. Date of publication August 12, 2016; date of current version November 18, 2016. Paper 2016-IDC-0292.R2, presented at the 2015 IEEE International Electric Machines and Drives Conference, Coeur d'Alene, ID, USA, May 11–13, and approved for publication in the IEEE Transactions on Industry Applications by the Industrial Drives Committee of the IEEE Industry Applications Society.

The authors are with the Institute of Electrical Machines, RWTH Aachen University, Aachen 52062, Germany (e-mail: Qian.Liu@iem.rwth-aachen.de; Kay.Hameyer@iem.RWTH-Aachen.DE).

Color versions of one or more of the figures in this paper are available online at http://ieeexplore.ieee.org.

Digital Object Identifier 10.1109/TIA.2016.2599902

In this paper, a method for the model predictive determination of the stator voltage vector including the optimized duty cycle is introduced for the DTC with MTPA. This basic idea was mentioned in the conference paper [25] and more details are given in this paper. The proposed scheme combines the FCSMPC and the Lyapunov theory. The cost function including the torque tracking, MTPA operation, and system constraints is utilized in this paper. The dominant part of the cost function is used as a Lyapunov function to calculate the duty cycle of each voltage vector in the finite set. The FCSMPC is implemented for a revised voltage set with the calculated duty cycles. After the execution of the FCSMPC, an optimum voltage can be obtained. With a complementary voltage, the proposed predictive control scheme has fixed switching frequency, which is realized by the SVPWM for both fast torque response and the minimization of the torque ripple.

II. PMSM and Inverter in dq Reference System

The proposed model predictive torque control is implemented in the *dq* reference coordinate system. The base frequency model of a PMSM described in the synchronous rotational *dq* coordinates is shown by the following equations:

$$\frac{di_d}{dt} = \frac{1}{L_d}(u_d - Ri_d + \omega L_q i_q) \tag{1}$$

$$\frac{di_q}{dt} = \frac{1}{L_q}(u_q - Ri_q - \omega L_d i_d - \omega \Psi_F) \tag{2}$$

$$T_e = 1.5\, p\,(\Psi_F + (L_d - L_q) i_d) i_q \tag{3}$$

where R, L_d, L_q, and Ψ_F are the stator resistance, inductance on *d*, *q*-axis, and the magnetic flux of the PMSM, respectively. p is the pole pair number. Using the forward euler approximation, the discrete current model of the PMSM is described by the following equation:

$$i_{d,k+1} = \left(1 - \frac{TR}{L_d}\right) i_{d,k} + \frac{T\omega L_q}{L_d} i_{q,k} + \frac{T}{L_d} u_{d,k} \tag{4}$$

$$i_{q,k+1} = \left(1 - \frac{TR}{L_q}\right) i_{q,k} - \frac{T\omega L_d}{L_q} i_{d,k} - \frac{T\omega \Psi_F}{L_q} + \frac{T}{L_q} u_{q,k} \tag{5}$$

where T is a small time interval, which can be smaller than or equal to the sampling time T_s.

The voltage of the PMSM $\boldsymbol{u}_{\mathrm{dq},k} = [u_{d,k}, u_{d,k}]^T$ is realized by the inverter. A two-level inverter has eight different switching status that $\{(S_a, S_b, S_c) \,|\, S_{a,b,c} \in \{0,1\}\}$, where S_a, S_b, and S_c are the switching status of the three phases, respectively. According to [26] and with the amplitude invariant Park transformation, the resulting voltage vectors in the *dq* coordinate system can be obtained by the following equation:

$$\begin{bmatrix} u_{d,k} \\ u_{q,k} \end{bmatrix} = \frac{2V_{\mathrm{DC}}}{3} \boldsymbol{M}_k \begin{bmatrix} 1 & -\frac{1}{2} & -\frac{1}{2} \\ 0 & \frac{\sqrt{3}}{2} & \frac{\sqrt{3}}{2} \end{bmatrix} \begin{bmatrix} S_{a,k} \\ S_{b,k} \\ S_{c,k} \end{bmatrix} \tag{6}$$

$$\boldsymbol{M}_k = \begin{bmatrix} \cos\Theta_k & \sin\Theta_k \\ -\sin\Theta_k & \cos\Theta_k \end{bmatrix}.$$

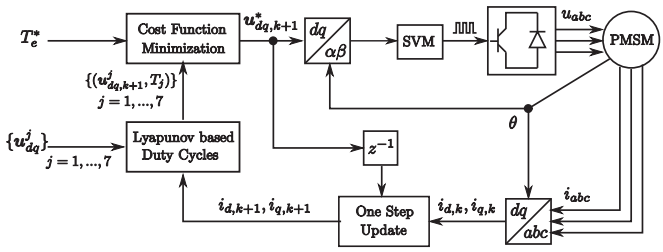

Fig. 1. Block diagram for the proposed FCSMPC strategy.

The eight switching states 0 0 0, 0 0 1 ...1 1 1 results in eight voltage vectors $\{\boldsymbol{u}^j_{\mathrm{dq},k} \,|\, j = 0, 1, \ldots, 7\}$ in the *dq* coordinate system. Since the switchings 0 0 0 and 1 1 1 have the same voltage vector, the voltage set $\{\boldsymbol{u}^j_{\mathrm{dq},k} \,|\, j = 1, \ldots, 7\}$ is considered for the MPC.

III. Torque Control With Modified FCSMPC Strategy

In order to minimize the current and torque ripples for the FCSMPC torque control, a Lyapunov based FCSMPC strategy is proposed in this section. The block diagram for the proposed FCSMPC strategy is shown in Fig. 1, which includes a one step update, a Lyapunov-based calculation of the duty cycles for the voltage set and the optimization of the control output voltage.

A. One Step Update

In the digital processor, the reference voltage can be only implemented to the inverter at the sampling instant. However, the calculation of the reference voltage costs some time so that the reference voltage can not be implemented on time. The principle of the delay from the digital processor is shown in Fig. 2(a). The subscript k denote the sampling instant and t_c is the calculation time of the reference voltage $\boldsymbol{u}^*_{\mathrm{dq},k}$. The state x_k denote the measurement at sampling instant k, which can be the torque or the current. The optimum voltage vector $\boldsymbol{u}^*_{\mathrm{dq},k}$ is obtained based on the measurement x_k and the predictive controller. Due to the calculation time t_c, the optimum reference voltage $\boldsymbol{u}^*_{\mathrm{dq},k}$ is implemented at the next sampling instant $k+1$. In this case, $\boldsymbol{u}^*_{\mathrm{dq},k}$ is no longer the optimum voltage vector for the state x_{k+1}, which results in additional ripples of the PMSM with FCSMPC [27].

In order to reduce the ripples from the one step calculation delay of the digital processor, a one step model-based update is taken into account. The principle of the one step update is shown in Fig. 2(b). The calculation time t_{c1} presents the one step update. Based on the voltage calculated from last step $k-1$, the measurement x_k and the model of the PMSM, the state at sampling instant $k+1$ can be updated and is denoted as x'_{k+1}. Based on the updated states, the optimum voltage $\boldsymbol{u}^*_{\mathrm{dq},k+1}$ can be obtained by the predictive controller with calculation time t_{c2}. With the one step delay of the digital processor, $\boldsymbol{u}^*_{\mathrm{dq},k+1}$ is implemented on time at sampling instant $k+1$. In this case, if the model of the PMSM is accurate enough, the reference voltage $\boldsymbol{u}^*_{\mathrm{dq},k+1}$ out of the predictive controller is the real optimum one for the real PMSM.

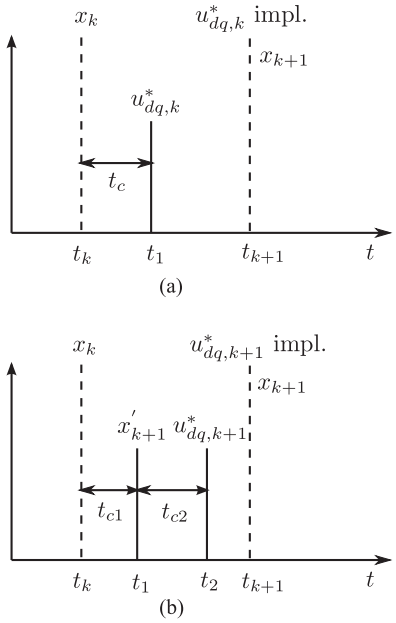

Fig. 2. Principle of the delay from the digital processor: (a) without update; (b) with one step update.

The one step update procedure is presented by the following equations:

$$i_{d,k+1} = \left(1 - \frac{T_s R}{L_d}\right) i_{d,k} + \frac{T_s \omega L_q}{L_d} i_{q,k} + \frac{T_s}{L_d} u^*_{d,k} \tag{7}$$

$$i_{q,k+1} = \left(1 - \frac{T_s R}{L_q}\right) i_{q,k} - \frac{T_s \omega L_d}{L_q} i_{d,k} - \frac{T_s \omega \Psi_F}{L_q} + \frac{T_s}{L_q} u^*_{q,k}. \tag{8}$$

The updated estimation $i_{d,k+1}$ and $i_{q,k+1}$ are utilized for the prediction process. The voltages $u^*_{d,k}$ and $u^*_{q,k}$ which are implemented by the inverter at sampling instant k are obtained from the last sampling instant $k-1$. The estimated torque $\hat{T}_{e,k+1}$ is calculated directly using (3).

B. Cost Function for the FCSMPC

In order to achieve the torque control with MTPA condition, a cost function considering the tracking of the torque, the MTPA operation, and the limitation of the current, which is similar to the one in [19], is utilized in this paper. The cost function is described by the following equations:

$$J(k+1) = \sum_{i=1}^{N_p} [k_T J_T(k+i) + k_A J_A(k+i) + k_L (J_{L1}(k+i) + J_{L2}(k+i))], \tag{9}$$

where N_p is the prediction length for the MPC. Since the FCSMPC is based on enumeration of the voltage vectors of the inverter, the computational cost of the FCSMPC increases exponentially with N_p. In order to realize real time calculation of FCSMPC, $N_p = 1$ is chosen in most of the literature [19], [20]. k_T, k_A, and k_L are the weighting factors of the cost function, which are positive real numbers. $J_T(k)$ and $J_A(k)$ denote the dominant objectives which are the torque dynamics and MTPA condition, respectively. The description of $J_T(k)$ and $J_A(k)$ are shown by the following equations:

$$J_T(k) = (T^*_e - \hat{T}_{e,k})^2 \tag{10}$$

$$J_A(k) = \left(i_{d,k} + \frac{L_d - L_q}{\Psi_F}(i^2_{d,k} - i^2_{q,k})\right)^2. \tag{11}$$

The current limitations of the PMSM are considered by $J_T(k)$ and $J_A(k)$ with following description:

$$J_{L1}(k) = \begin{cases} 0, & \text{if } I_r \le \sqrt{i^2_{d,k} + i^2_{d,k}} \\ \left(I_r - \sqrt{i^2_{d,k} + i^2_{d,k}}\right)^2, & \text{otherwise} \end{cases}$$

$$J_{L2}(k) = \begin{cases} 0, & \text{if } i_{d,k} \le 0 \\ i^2_{d,k}, & \text{otherwise} \end{cases}$$

where I_r is the rated current of the PMSM. $J_{L1}(k)$ denotes the current limit due to the thermal consideration. J_{L2} is to ensure that the d-axis current i_d converges to the correct solution for the MTPA condition. With the help of the cost function, the torque control with MTPA condition is transformed to minimize the cost function $J(k+2)$. In the cost function, k_L is much larger than k_T and k_A to prevent the PMSM from over current and to make sure $i_d \le 0$. For the choice of k_T and k_A, $k_T + k_A = 1$ can be imposed. Large k_T leads to fast torque convergence, while large k_A stands for fast convergence of the MTPA condition. In order to achieve fast torque response, $k_T > k_A$ can be chosen.

C. Calculation of the Duty Cycles

In order to minimize the current and torque ripple of the PMSM with FCSMPC, a Lyapunov function is proposed to introduce a duty cycle for each voltage vector in the finite set. Since the current limitations J_{L1} and J_{L2} are only constraints and are not globally differentiable, they are not considered in the Lyapunov function for the calculation of the duty cycles. The proposed Lyapunov function is chosen as the dominant objectives in the cost function with $N_p = 1$, which is shown by the following equation:

$$V(k+1) = k_T J_T(k+1) + k_A J_A(k+1). \tag{12}$$

When the condition $V(k) = 0$ holds, the torque $T'_{e,k} = T^*_e$ and the MTPA condition of the PMSM can be reached at time instant k. Furthermore, when $\frac{dV(k)}{dt} = 0$ is fulfilled, the transient torque and flux will be stabilized at the optimum MTPA operating point so that the current and torque ripples can be minimized.

The Lyapunov-based duty cycles are to realize the first condition $V(k) = 0$ with the voltage vectors in the finite set. The following property holds for the MTPA condition:

Lemma 3.1: Defining $f(i_d, i_q) = i_d + \frac{L_d - L_q}{\Psi_F}(i^2_d - i^2_q)$ is a function of the current. If the torque of the PMSM is kept at a nonzero constant value, $f(i_d, i_q)$ is a strict monotonic function along the constant torque curve.

Lemma 3.1 is proven in Appendix A. With the help of this lemma, the Lyapunov function is strictly decreasing if the

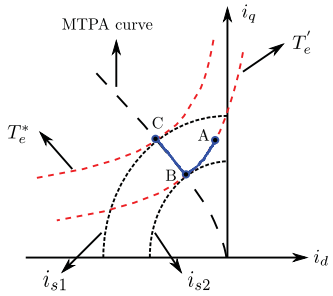

Fig. 3. Current loci of the MTPA condition.

current trajectory is controlled as following: first along the constant torque curve until the MTPA curve $f(i_d, i_q) = 0$ is reached; then along the MTPA curve to the operating point with $V = 0$. An example is shown in Fig. 3. At the initial point A, the trajectory is along $\overrightarrow{AB}$ and $\overrightarrow{BC}$. Therefore, there exists at least one current trajectory which decreases the Lyapunov function (12). Consequently, the following Lemma holds:

Lemma 3.2: For each initial condition of the PMSM, if the back-emf of the PMSM is within the voltage limitation of the inverter, there exists a feasible voltage vector $\boldsymbol{u}^*_{\mathrm{dq},k+1}$ which fulfills $\frac{dV(k+1)}{dt} \leq 0$.

The proof of *Lemma 3.1* can be found in Appendix B. Moreover, similar to the Lemma 5.1 in [28], the following lemma also holds for the voltage vectors of the a 2-level converter:

Lemma 3.3: For the given current dynamics

$$\frac{d\boldsymbol{i}_{\mathrm{dq},k+1}}{dt} = \boldsymbol{A}\boldsymbol{i}_{\mathrm{dq},k+1} + \boldsymbol{B}\boldsymbol{u}_{\mathrm{dq},k+1} + \boldsymbol{E} \tag{13}$$

if the back-emf of the PMSM is within the voltage limitation of the inverter, there exists at least one votlage vector $\boldsymbol{u}^a_{\mathrm{dq},k+1}$ with $a \in \{1, \ldots, 7\}$, which fulfills

$$\frac{V_a(k+1)}{dt} = \frac{\partial V(k+1)}{\partial \boldsymbol{i}_{\mathrm{dq},k+1}}(\boldsymbol{A}\boldsymbol{i}_{\mathrm{dq},k+1} + \boldsymbol{B}\boldsymbol{u}^a_{\mathrm{dq},k+1} + \boldsymbol{E}) \leq 0. \tag{14}$$

The definition of $\boldsymbol{A}$, $\boldsymbol{B}$, and $\boldsymbol{E}$ is shown in Appendix D. The proof of *Lemma 3.3* can be referred to *Lemma 3.2* and the proof of the *Lemma 5.1* in [28].

In order to minimize the current and torque ripple of the PMSM, it is expected that the Lyapunov function stay at $V = 0$ and $\frac{dV}{dt} = 0$ in the steady state. The following calculation of the duty cycle for each voltage vector $\boldsymbol{u}^j_{\mathrm{dq},k+1}$ are introduced to fulfill this expectation:

$$T^j_{\mathrm{duty},k+1} = \begin{cases} T_\sigma, & \text{if } \dfrac{dV_j(k+1)}{dt} > 0 \\ 0, & \text{if } \dfrac{dV_j(k+1)}{dt} = 0 \\ \dfrac{-V(k+1)}{dV_j(k+1)/dt}, & \text{otherwise} \end{cases} \tag{15}$$

where $T_\sigma \ll T_s$ is a constant. T_σ is introduced for the situation that the current limit is reached. In this case, the current limit J_L becomes important in the cost function. The voltage vector with $\frac{dV_j(k+1)}{dt} > 0$ also has to be taken into account in the FCSMPC. However, it is expected that such voltage vector does not diverge the Lyapunov function V too much. When the PMSM model and the prediction are accurate, $T_\sigma = 0$ is the ideal value for the ripple reduction. However, in the real PMSM system, there is disturbance due to the variation of machine parameters and the voltage error in the inverter. Therefore, a small T_σ is chosen to compromise the disturbance, which can be different for each PMSM system. $T_\sigma = 0.1T_s$ is utilized in this paper for a certain degree of safety margin. However, it can be improved by the testing of T_σ for a specific PMSM system.

The calculated duty cycle T^j_{duty} is limited to $[0\ T_s]$. With the help of *Lemma 3.3*, it can be noticed that at each time step $k+1$ without considering the current constraints, there is at least one voltage vector $u^a_{\mathrm{dq},k+1}$ with its duty cycle $T^a_{\mathrm{duty},k+1}$ to ensure the Lyapunov function $V(k+2) = J(k+2)$ to converge towards 0. On the other hand, the calculated duty cycle $T^a_{\mathrm{duty},k+1}$ using (15) can be used to keep $\frac{dV}{dt} = 0$ in the steady state, which will be shown in the following section. Therefore, all voltage vectors $u^j_{\mathrm{dq},k+1}$ with $\frac{dV_j(k+1)}{dt} < 0$ are the candidates to minimize that the cost function $J(k+2)$. Considering the case that the system constraints of the PMSM, a revised finite set $\{(u^j_{\mathrm{dq},k+1}, T^j_{\mathrm{duty},k+1}) \,|\, j = 1, 2, , 7\}$ with duty cycles is applied to the FCSMPC.

D. Implementation of the FCSMPC

To implement the FCSMPC with the revised finite set, a supplement voltage vector is defined for the control with fixed sampling rate and switching frequency

$$\boldsymbol{u}^s_{\mathrm{dq},k+1} = \begin{bmatrix} Ri_{d,k+1} - \omega L_q i_{q,k+1} \\ Ri_{q,k+1} + \omega L_d i_{d,k+1} + \omega \Psi_F. \end{bmatrix}. \tag{16}$$

It can be noticed that with the supplement voltage, the derivative of the current $\frac{d\boldsymbol{i}_{\mathrm{dq},k+1}}{dt}$ is 0 so that the cost function does not change. Defining a voltage

$$\boldsymbol{u}_{\mathrm{dq},k+1} = \left(1 - \frac{T^j_{\mathrm{duty},k+1}}{T_s}\right)\boldsymbol{u}^s_{\mathrm{dq},k+1} + \frac{T^j_{\mathrm{duty},k+1}}{T_s}\boldsymbol{u}^j_{\mathrm{dq},k+1}. \tag{17}$$

The duration of the voltage vector $\boldsymbol{u}_{\mathrm{dq},k+1}$ is one sampling time T_s. When the voltage $\boldsymbol{u}_{\mathrm{dq},k+1}$ is applied to the PMSM, only the voltage vector $\boldsymbol{u}^j_{\mathrm{dq},k+1}$ with its duty cycle $T^j_{\mathrm{duty},k+1}$ are effective on the current and torque of the PMSM. It guarantees the convergence of the torque and the MTPA condition. Afterward, the supplement voltage $\boldsymbol{u}^s_{\mathrm{dq},k+1}$ with duration $T_s - T^j_{\mathrm{duty},k+1}$ leads to $\frac{dV}{dt} = 0$.

The $\boldsymbol{u}^j_{\mathrm{dq},k+1}$ in the voltage finite set is determined after the FCSMPC. In order to obtain a more precise prediction and for the system optimality, the revised finite set with duty cycles are implemented to the FCSMPC. The current at time point t_{k+2} with each voltage vector $\boldsymbol{u}^j_{\mathrm{dq},k+1}$ can be calculated by the

following equation:

$$i^j_{d,k+2} = \left(1 - \frac{T^j_{\text{duty},k+1}R}{L_d}\right) i_{d,k+1} + \frac{T^j_{\text{duty},k+1}\omega L_q}{L_d} i_{q,k+1} + \frac{T^j_{\text{duty},k+1}}{L_d} u^j_{d,k+1} \tag{18}$$

$$i^j_{q,k+2} = \left(1 - \frac{T^j_{\text{duty},k+1}R}{L_q}\right) i_{q,k+1} + \frac{T^j_{\text{duty},k+1}\omega L_d}{L_q} i_{d,k+1} - \frac{T^j_{\text{duty},k+1}\omega \Psi_F}{L_q} + \frac{T^j_{\text{duty},k+1}}{L_q} u^j_{q,k+1}. \tag{19}$$

With the predicted current, the optimum index of the voltages is obtained by evaluating the cost function

$$b = \arg \min_{j\in\{1,\ldots,7\}} \{J^j(k+2)\}. \tag{20}$$

The optimum output reference voltage is:

$$\boldsymbol{u}^*_{\text{dq},k+1} = \left(1 - \frac{T^b_{\text{duty},k+1}}{T_s}\right) \boldsymbol{u}^s_{\text{dq},k+1} + \frac{T^b_{\text{duty},k+1}}{T_s} \boldsymbol{u}^b_{\text{dq},k+1} \tag{21}$$

which is realized by the SVPWM. From (21), it can be noticed that with the proposed FCSMPC, the optimum duty cycle $T^b_{\text{duty},k+1}$ can equal to T_s to minimize the cost function during the transient operation. Therefore, the torque response of the proposed strategy is as fast as the standard FCSMPC if they are using the same sampling time. Lemma 3.3 guarantees the stability of the proposed control scheme. On the other hand, during the steady state, the supplement voltage keeps the derivative $\frac{dV}{dt} = 0$ if $V = 0$ is reached. Therefore, the current and torque ripple can be minimized. For the proposed strategy, the derivative of the Lyapunov function has to be calculated for seven voltage vectors for the proposed strategy. The computation time can be approximately doubled when compared to the standard FCSMPC. However, the sampling frequency for the proposed FCSMPC strategy can be much smaller than the standard one.

IV. Simulation Results

The simulation model is implemented in MATLAB/Simulink to validate the performance of proposed control scheme. The nominal parameters of the IPMSM are collected in Appendix C. The speed of the machine is controlled to 300 r/min. The proposed control scheme is compared to the model predictive torque control with standard FCSMPC described in [19] without error rejection. The weighting factors in the cost function for both proposed and standard FCSMPC are set to $k_T = 0.8$, $k_A = 0.2$, and $k_L = 100$. The time constant T_σ is set to $0.1T_s$.

For the torque control with standard FCSMPC, the sampling frequency of the system is set to 30 kHz. The average switching frequency of the inverter is calculated by counting the number of switching in 0.02 s and dividing by the factor 6. So the calculated switching frequency is comparable to the symmetric SVPWM. The simulation results for the torque control with standard FCSMPC and without parameter error are shown in Fig. 4. It can be noticed that the switching frequency is slightly above 4 kHz. The simulation results for the torque control with proposed control strategy are shown in Fig. 5. The sampling frequency of the system and the carrier frequency of the SVPWM for the proposed control strategy are both set to 4 kHz. Comparing the simulation results in Figs. 4 and 5, it can be noticed that both methods realize the DTC and the MTPA condition. The torque response with the proposed FCSMPC is slightly slower than the

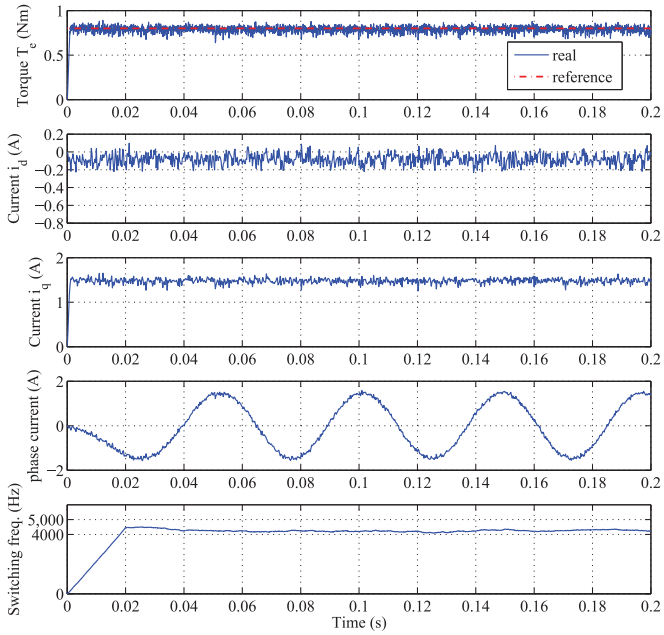

Fig. 4. Simulation results for the torque control with standard FCSMPC without parameter error.

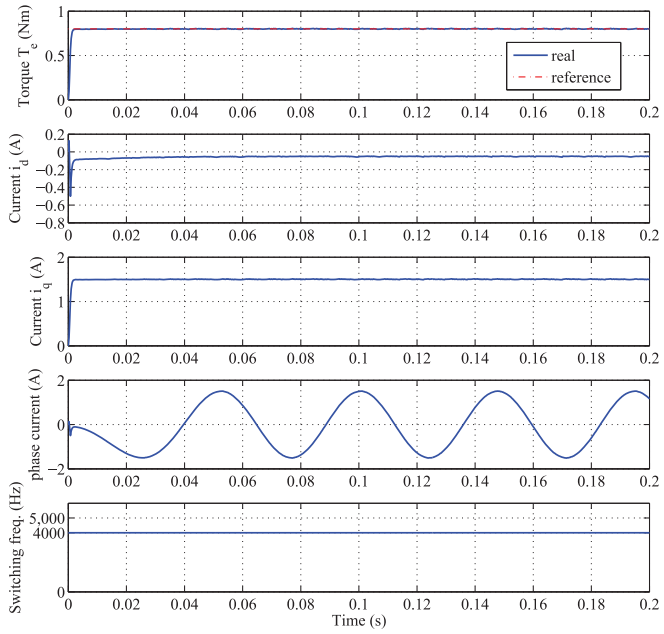

Fig. 5. Simulation results for the torque control with proposed FCSMPC without parameter error.

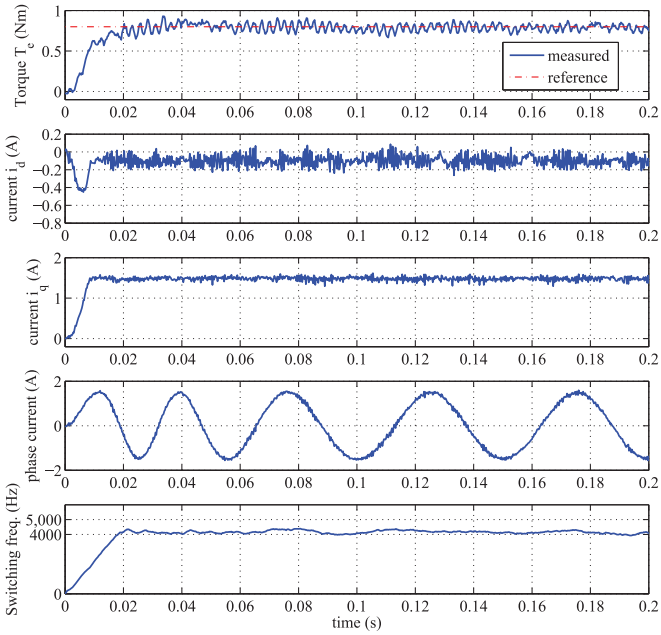

Fig. 6. Experimental results for the torque control with standard FCSMPC without parameter error.

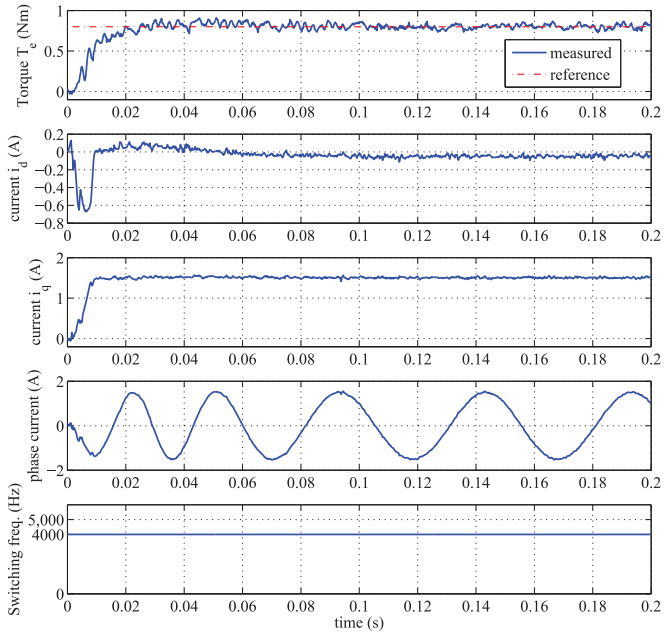

Fig. 7. Experimental results for the torque control with proposed FCSMPC without parameter error.

one with the standard FCSMPC, since the sampling frequency of the proposed FCSMPC is slower. However, the current and torque ripples of the PMSM with proposed FCSMPC are minimized in the ideal case, which are much smaller than the one with standard FCSMPC.

V. Experimental Results

To verify the feasibility of the proposed control strategy in the reality, several experiments are performed by using the PMSM with parameters from Appendix C. The controller is implemented in the dSPACE rapid control prototyping system (DS1103). The configuration of the controller for the proposed control strategy in the experiments is set as the same as the one for the simulation in Section IV. The sampling frequency for the standard FCSMPC is set to 32 kHz to achieve the switching frequency 4 kHz. The speed of the IPMSM is controlled at the speed 300 r/min by a load machine. In order to make a fair comparison, the experimental results of the standard FCSMPC are shown with the down sampling frequency 4 kHz, which is the same with the proposed one.

The experimental results without parameter error for the torque control with standard and proposed FCSMPC are shown in Figs. 6 and 7, respectively. It can be noticed that the torque response of the standard and proposed control strategy are approximately the same. On the other hand, with the same average switching frequency, the current and torque ripples for the proposed control strategy are much smaller than the standard one due to the introduced duty cycles.

In order to investigate the sensitivity of the parameter error for the proposed control strategy, two types parameter errors which have large influence on the PMSM stability are imposed to the experiments. For the inductance, L_d and L_q have similar effects in the PMSM model and the cost function. Moreover, in the real PMSM, the saturation effect in L_d is much smaller than one in L_q. The experiment with L_q error is sufficient to show the case with inductance error. The parameter errors are introduced by using the wrong parameters $1.5L_q$ and $1.3\Psi_F$ for the controller, respectively. The experimental results with parameter error $1.5L_q$ are shown in Figs. 8 and 9. The torque control with both standard and proposed FCSMPC has approximately the same steady-state operating. From the experimental results, it is shown that the L_q error has only small influence on the proposed torque control strategy. In Fig. 9, the operating point deviates from the optimum MTPA condition due to the parameter error. However, the torque of the PMSM has very small displacement from the reference value. When compared to the experimental results for the standard FCSMPC in Fig. 8, the current and torque ripples are still much smaller for the proposed control strategy with inductance error. On the other hand, when compared to the results for the no error case in Fig. 7, the influences of the inductance error on the current and torque ripples are limited.

The experimental results with $1.3\Psi_F$ are shown in Figs. 10 and 11. It can be noticed that the flux error has relatively larger impact on the torque control when compared to the inductance error. In Fig. 10, it can be noticed that steady-state torque error exists for the proposed torque control strategy and the operating point deviates from the MTPA condition due to the flux error. However, the torque error is smaller than the one with standard FCSMPC in Fig. 11. When compared to the one without parameter error in Fig. 7, the torque ripple increases for the proposed control strategy, which is approximately the same as

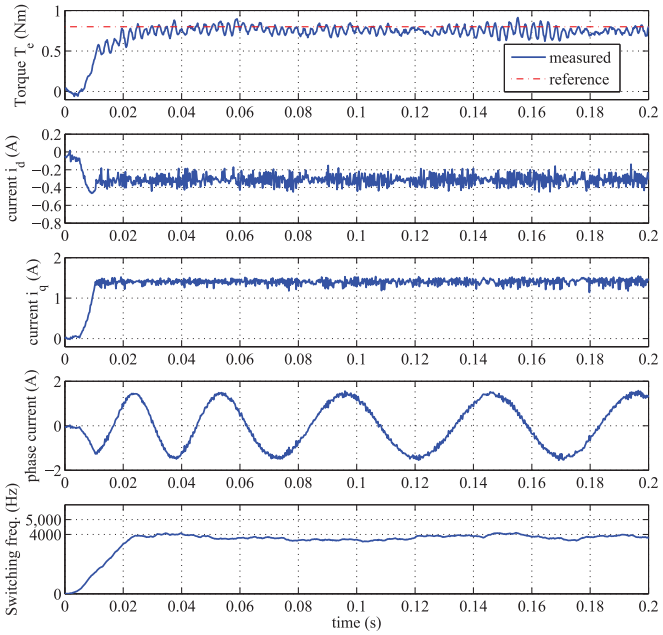

Fig. 8. Experimental results for the torque control with standard FCSMPC with parameter error $1.5L_q$.

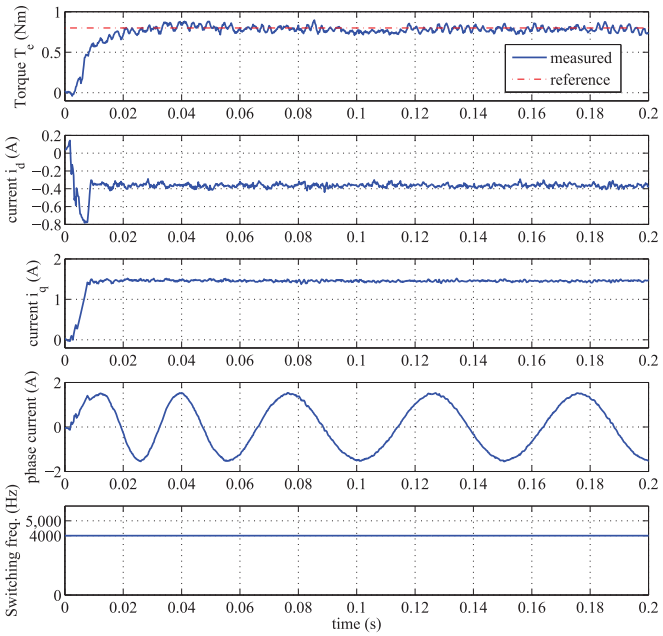

Fig. 9. Experimental results for the torque control with proposed FCSMPC with parameter error $1.5L_q$.

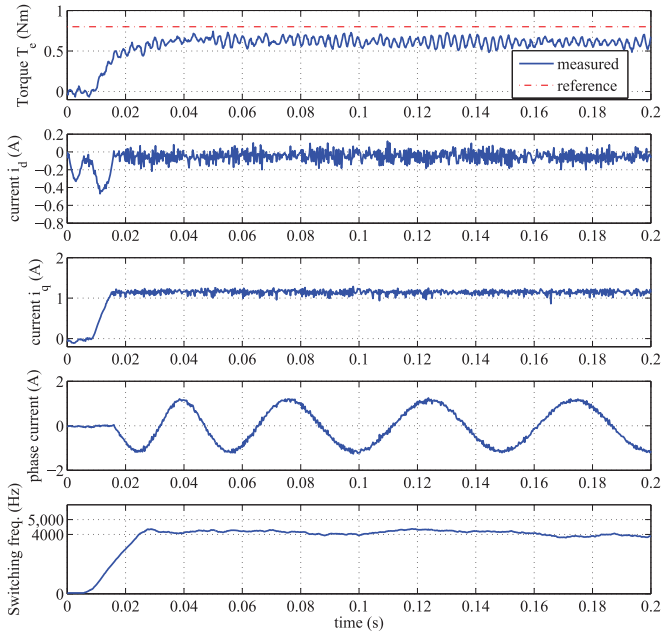

Fig. 10. Experimental results for the torque control with standard FCSMPC with parameter error $1.3\Psi_F$.

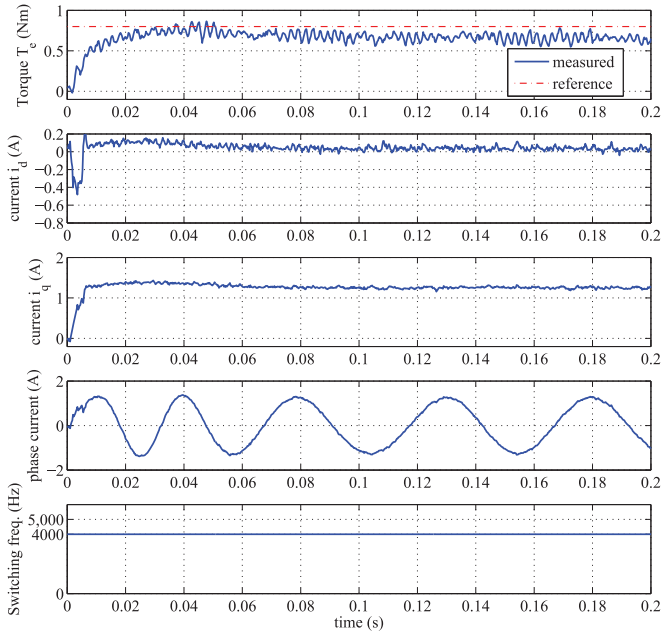

Fig. 11. Experimental results for the torque control with proposed FCSMPC with parameter error $1.3\Psi_F$.

the torque ripple with standard FCSMPC in Fig. 10. However, the increment of the current ripples is small for the proposed strategy with flux error, which is much smaller than the standard case.

From Figs. 6–11, the torque responses in the experiments are much smaller than the one in the simulation for both standard and proposed. This is due to the voltage error from the inverter. With voltage error, the prediction in the FCSMPC is inaccurate so that the selected voltage vector may not be the real optimum one. It slows the dynamics of the torque responses and results in similar torque dynamics for both standard and proposed FCSMPC. Fig. 12 shows an overview of the spectrum for the current and torque in the experiments. In all cases with and without parameter errors, both torque and current harmonics of proposed FCSMPC are much smaller when compared

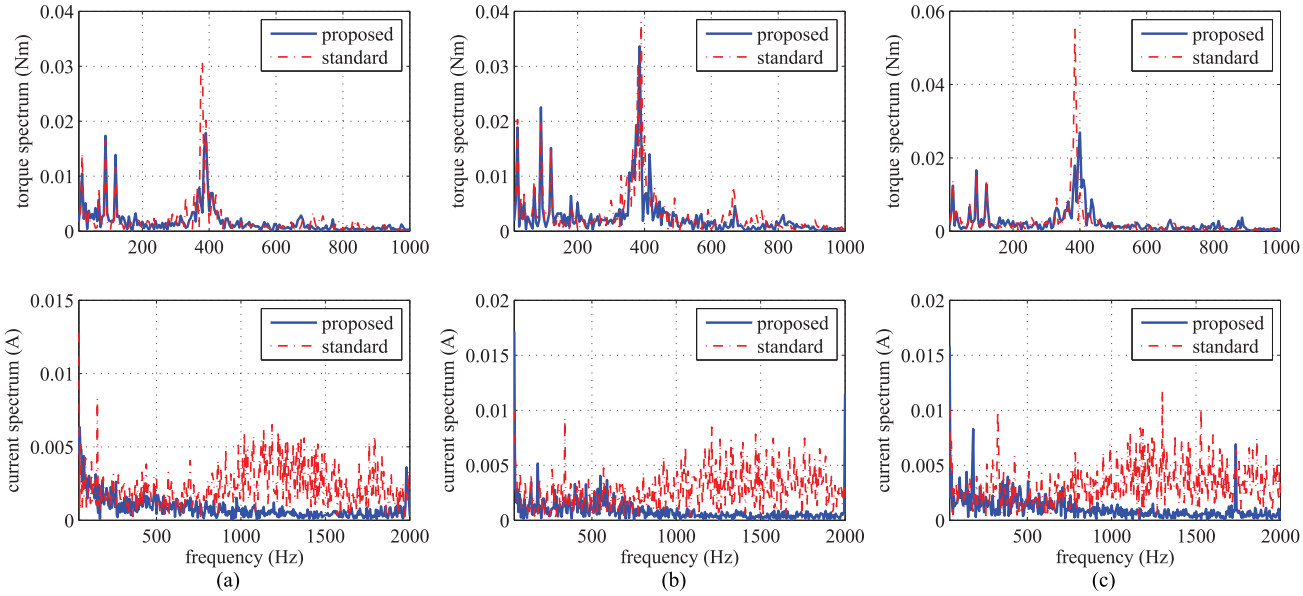

Fig. 12. Torque and current spectrum of the experimental results: (a) no parameter error; (b) with parameter error 1.5 L_q; (c) with parameter error 1.3 Ψ_F.

to the one with standard FCSMPC. With the comparisons discussed above, it is shown that the performance of the torque control with proposed FCSMPC holds better performance than the standard FCSMPC with and without parameter errors. To increase the robustness for the proposed control scheme, it is also possible to introduce a model error compensation with Kalman or Adaptive Observer to reduce the steady-state error and ripples.

VI. Conclusion

In this paper, a Lyapunov-based model predictive DTC (FCSMPC) with MTPA for the PMSM is proposed. The natural characteristics of the two-level converter which are the eight voltage vectors are used to obtain an optimum voltage for the PMSM. A Lyapunov-based duty cycle for each voltage vector is introduced for the implementation of the FCSMPC. A cost function including the torque tracking, the attraction of the MTPA region, and the current limitation is utilized for the FCSMPC. Before the FCSMPC, the dominant part of the aforementioned cost function is used as a Lyapunov function to calculate the desired duty cycle for each voltage vector. Theoretical conclusions are shown and proved for the feasibility, stability, and performance analysis of the calculated duty cycles. An optimum voltage can be obtained by combining the FCSMPC with a revised finite set of the seven different voltage vectors with their duty cycles and a supplement voltage. The proposed control scheme can realize a small sampling frequency, fixed switching frequency, and torque ripple minimization. The experimental results show the good performance of the proposed control scheme and the sensitivity of the parameter errors is investigated. The torque and current ripples can be significantly reduced when compared to the torque control with standard FCSMPC.

Appendix A
Proof of Lemma 3.1

The conditions of *Lemma 3.1* can be described by the following equations:

$$f(i_d, i_q) = i_d + \frac{L_d - L_q}{\Psi_F}(i_d^2 - i_q^2) \tag{22}$$

$$T_e = 1.5\, p\, [\Psi_F + (L_d - L_q) i_d] i_q = \text{const.} \tag{23}$$

Taking the partial derivatives based on the current vector $\boldsymbol{i}_{\mathrm{dq}}$, we have

$$\frac{\partial f(i_d, i_q)}{\partial \boldsymbol{i}_{\mathrm{dq}}} = \left[1 + \frac{2(L_d - L_q)}{\Psi_F} i_d, -\frac{2(L_d - L_q)}{\Psi_F} i_q\right] \tag{24}$$

$$\frac{\partial T_e}{\partial \boldsymbol{i}_{\mathrm{dq}}} = [1.5\, p\, (L_d - L_q) i_q,\ 1.5\, p\, (\Psi_F + (L_d - L_q) i_q)]. \tag{25}$$

When the torque T_e remains constant, the trajectory of the operating point moves along the direction of the vector $\boldsymbol{r}$ which fulfills $\frac{\partial T_e}{\partial \boldsymbol{i}_{\mathrm{dq}}} \boldsymbol{r} = 0$. The vector $\boldsymbol{r}$ can be presented by the following form:

$$\boldsymbol{r} = \epsilon[-1.5\, p\, (\Psi_F + (L_d - L_q) i_q),\ 1.5\, p\, (L_d - L_q) i_q]^T \tag{26}$$

where ϵ is a positive real number. It can be noticed that

$$\frac{\partial f(i_d, i_q)}{\partial \boldsymbol{i}_{\mathrm{dq}}} \boldsymbol{r} = 1.5 p \epsilon [\Psi_F + 3(L_d - L_q) i_d] - \frac{3 p \epsilon (L_d - L_q)^2}{\Psi_F}(i_d^2 + i_q^2). \tag{27}$$

Since $L_d - L_q \leq 0$ and $i_d \leq 0$ hold for the PMSM, $\frac{\partial f(i_d, i_q)}{\partial \boldsymbol{i}_{\mathrm{dq}}} \boldsymbol{r} < 0$ is true. Therefore, the function $f(i_d, i_q)$ is monotonic along the constant torque curve.

APPENDIX B
PROOF OF LEMMA 3.2

Considering the derivative of the Lyapunov function

$$\frac{dV(k+1)}{dt} = \frac{\partial V(k+1)}{\partial \boldsymbol{i}_{\mathrm{dq},k+1}} \frac{d\boldsymbol{i}_{\mathrm{dq},k+1}}{dt} \tag{28}$$

where $\boldsymbol{i}_{\mathrm{dq},k+1}$ is the current vector. Since there exists a current trajectory so that $V(k+1)$ is decreasing, there exists $\Delta \boldsymbol{i}_{\mathrm{dq},k+1}$ which fulfills

$$\frac{\partial V(k+1)}{\partial \boldsymbol{i}_{\mathrm{dq},k+1}} \Delta \boldsymbol{i}_{\mathrm{dq},k+1} \leq 0. \tag{29}$$

The equal holds if and only if the $V(k+1) = 0$ is reached. Therefore, there exists a current derivative $\frac{d\boldsymbol{i}_{\mathrm{dq},k+1}}{dt} = \epsilon \Delta \boldsymbol{i}_{\mathrm{dq},k+1}$ so that $\frac{dV(k+1)}{dt} \leq 0$ holds. Here ϵ can be a very small positive constant. Considering the voltage $\boldsymbol{u}_{\mathrm{dq},k+1}$ which fulfills

$$\boldsymbol{u}_{\mathrm{dq},k+1} = \boldsymbol{L} \frac{d\boldsymbol{i}_{\mathrm{dq},k+1}}{dt} + \boldsymbol{u}_E = \epsilon \boldsymbol{L} \Delta \boldsymbol{i}_{\mathrm{dq},k+1} + \boldsymbol{u}_E \tag{30}$$

where $\boldsymbol{L}$ and $\boldsymbol{u}_E$ are

$$\boldsymbol{L} = \begin{bmatrix} L_d & 0 \\ 0 & L_q \end{bmatrix}, \ \boldsymbol{u}_E = \begin{bmatrix} Ri_{d,k+1} - \omega L_q i_{q,k+1} \\ Ri_{q,k+1} + \omega(L_d i_{d,k+1} + \Psi_F) \end{bmatrix}.$$

When $\boldsymbol{u}_E$ is within the voltage limit of the inverter, ϵ can be chosen small enough to ensure $\boldsymbol{u}_{\mathrm{dq},k+1}$ is within the voltage limit of the inverter. It can be easily noticed that such $\boldsymbol{u}_{\mathrm{dq},k+1}$ guarantees $\frac{dV(k+1)}{dt} \leq 0$.

APPENDIX C
PARAMETERS OF THE PMSM

Rated current	$i_{\max}$	2.3 A
Rated torque	$T_{\max}$	1.23 Nm
DC-link voltage	V_{DC}	60 V
Pole pair number	p	4
Stator resistance	R	3.3 Ω
d-axis inductance	L_d	16 mH
q-axis inductance	L_q	20 mH
Flux linkage	Ψ_F	0.0886 Vs/rad

APPENDIX D
DEFINITION OF MATRICES

$$\boldsymbol{A} = \begin{bmatrix} -\frac{R}{L_d} & \frac{\omega L_q}{L_d} \\ -\frac{\omega L_d}{L_q} & -\frac{R}{L_q} \end{bmatrix}, \ \boldsymbol{B} = \begin{bmatrix} \frac{1}{L_d} & 0 \\ 0 & \frac{1}{L_q} \end{bmatrix}, \ \boldsymbol{E} = \begin{bmatrix} 0 \\ -\frac{\omega \Psi_F}{L_q} \end{bmatrix}.$$

REFERENCES

[1] H. Zhu, X. Xiao, and Y. Li, "Torque ripple reduction of the torque predictive control scheme for permanent-magnet synchronous motors," *IEEE Trans. Ind. Electron.*, vol. 59, no. 2, pp. 871–877, Feb. 2012.

[2] M. Rahman and L. Zhong, "Comparison of torque responses of the interior permanent magnet motor under pwm current and direct torque controls," in *Proc. 25th Annu. Conf. IEEE Ind. Electron. Soc.*, 1999, vol. 3, pp. 1464–1470.

[3] F. Niu, B. Wang, A. S. Babel, K. Li, and E. G. Strangas, "Comparative evaluation of direct torque control strategies for permanent magnet synchronous machines," *IEEE Trans. Power Electron.*, vol. 31, no. 2, pp. 1408–1424, Feb. 2016.

[4] G. Foo and M. Rahman, "Direct torque control of an ipm-synchronous motor drive at very low speed using a sliding-mode stator flux observer," *IEEE Trans. Power Electron.*, vol. 25, no. 4, pp. 933–942, Apr. 2010.

[5] M. N. Uddin, H. Zou, and F. Azevedo, "Online loss-minimization-based adaptive flux observer for direct torque and flux control of PMSM drive," *IEEE Trans. Ind. Appl.*, vol. 52, no. 1, pp. 425–431, Jan. 2016.

[6] D. Swierczynski, M. Kazmierkowski, and F. Blaabjerg, "DSP based direct torque control of permanent magnet synchronous motor (PMSM) using space vector modulation (DTC-SVM)," in *Proc. IEEE Int. Symp. Ind. Electron.*, 2002, vol. 3, pp. 723–727.

[7] L. Tang, L. Zhong, M. Rahman, and Y. Hu, "A novel direct torque controlled interior permanent magnet synchronous machine drive with low ripple in flux and torque and fixed switching frequency," *IEEE Trans. Power Electron.*, vol. 19, no. 2, pp. 346–354, Mar. 2004.

[8] Y. Cho, K.-B. Lee, J.-H. Song, and Y. Lee, "Torque-ripple minimization and fast dynamic scheme for torque predictive control of permanent-magnet synchronous motors," *IEEE Trans. Power Electron.*, vol. 30, no. 4, pp. 2182–2190, Apr. 2015.

[9] M. H. Vafaie, B. M. Dehkordi, P. Moallem, and A. Kiyoumarsi, "A new predictive direct torque control method for improving both steady-state and transient-state operations of the pmsm," *IEEE Trans. Power Electron.*, vol. 31, no. 5, pp. 3738–3753, May 2016.

[10] Y. Zhang and J. Zhu, "Direct torque control of permanent magnet synchronous motor with reduced torque ripple and commutation frequency," *IEEE Trans. Power Electron.*, vol. 26, no. 1, pp. 235–248, Jan. 2011.

[11] J. S. Lee, R. D. Lorenz, and M. A. Valenzuela, "Time-optimal and loss-minimizing deadbeat-direct torque and flux control for interior permanent-magnet synchronous machines," *IEEE Trans. Ind. Appl.*, vol. 50, no. 3, pp. 1880–1890, May 2014.

[12] W. Xu and R. D. Lorenz, "Dynamic loss minimization using improved deadbeat-direct torque and flux control for interior permanent-magnet synchronous machines," *IEEE Trans. Ind. Appl.*, vol. 50, pp. 1053–1065, Mar. 2014.

[13] Y. Chen, D. Sun, B. Lin, T. W. Ching, and W. Li, "Dead-beat direct torque and flux control based on sliding-mode stator flux observer for pmsm in electric vehicles," in *Proc. 41st Annu. Conf. IEEE Ind. Electron. Soc.*, Nov. 2015, pp. 002270–002275.

[14] P. Cortes "Guidelines for weighting factors design in model predictive control of power converters and drives," in *Proc. IEEE Int. Conf. Ind. Technol.*, 2009, pp. 1–7.

[15] J. Rodriguez, "State of the art of finite control set model predictive control in power electronics," *IEEE Trans. Ind. Informat.*, vol. 9, no. 2, pp. 1003–1016, May 2013.

[16] W. Xie, "Finite control set-model predictive torque control with a deadbeat solution for PMSM drives," *IEEE Trans. Ind. Electron.*, vol. 62, no. 9, pp. 5402–5410, Sep. 2015.

[17] W. Xie, X. Wang, F. Wang, W. Xu, R. Kennel, and D. Gerling, "Dynamic loss minimization of finite control set-model predictive torque control for electric drive system," *IEEE Trans. Power Electron.*, vol. 31, no. 1, pp. 849–860, Jan. 2016.

[18] J. Rodriguez, P. Cortes, R. Kennel, and M. Kazrnierkowski, "Model predictive control – A simple and powerful method to control power converters," in *Proc. IEEE 6th Int. Power Electron. Motion Control Conf.*, 2009, pp. 41–49.

[19] M. Preindl and S. Bolognani, "Model predictive direct torque control with finite control set for PMSM drive systems, part 1: Maximum torque per ampere operation," *IEEE Trans. Ind. Informat.*, vol. 9, no. 4, pp. 1912–1921, Nov. 2013.

[20] A. Mora, A. Orellana, J. Juliet, and R. Cardenas, "Model predictive torque control for torque ripple compensation in variable speed PMSMs." *IEEE Trans. Ind. Electron.*, vol. 63, no. 7, pp. 4584–4592, Jul. 2016.

[21] Z. Ma, S. Saeidi, and R. Kennel, "FPGA implementation of model predictive control with constant switching frequency for PMSM drives," *IEEE Trans. Ind. Informat.*, vol. 10, no. 4, pp. 2055–2063, Nov. 2014.

[22] S. Wang, C. Xia, X. Gu, and W. Chen, "A novel FCS-model predictive control algorithm with duty cycle optimization for surface-mounted PMSM," in *Proc. 7th IET Int. Conf. Power Electron., Mach. Drives*, 2014, pp. 1–6.

[23] Y. Zhang and X. Wei, "Torque ripple RMS minimization in model predictive torque control of PMSM drives," in *Proc. Int. Conf. Elect. Mach. Syst.*, 2013, pp. 2183–2188.

[24] Y. Zhang and S. Gao, "Simultaneous optimization of voltage vector and duty cycle in model predictive torque control of PMSM drives," in *Proc. 17th Int. Conf. Elect. Mach. Syst.*, 2014, pp. 3338–3344.
[25] Q. Liu and K. Hameyer, "A finite control set model predictive direct torque control for the PMSM with MTPA operation and torque ripple minimization," in *Proc. IEEE Int. Elect. Mach. Drives Conf.*, May 2015, pp. 804–810.
[26] F. Morel, X. Lin-Shi, J.-M. Retif, B. Allard, and C. Buttay, "A comparative study of predictive current control schemes for a permanent-magnet synchronous machine drive," *IEEE Trans. Ind. Electron.*, vol. 56, no. 7, pp. 2715–2728, Jul. 2009.
[27] P. Cortes, J. Rodriguez, C. Silva, and A. Flores, "Delay compensation in model predictive current control of a three-phase inverter," *IEEE Trans. Ind. Electron.*, vol. 59, no. 2, pp. 1323–1325, Feb. 2012.
[28] G. Prior and M. Krstic, "Quantized-input control lyapunovapproach for permanent magnet synchronous motor drives," *IEEE Trans. Control Syst. Technol.*, vol. 21, no. 5, pp. 1784–1794, Sep. 2013.

Qian Liu received the Bachelor's degree in electrical engineering from Shanghai Jiao Tong University, Shanghai, China, in 2008, and the Master degree in control engineering from Technical University of Kaiserslautern, Kaiserslautern, Germany. He is currently a Research Associate in the Institute of Electrical Machines, RWTH Aachen University, Aachen, Germany. His research interests include high performance PMSM drive system and power electronics in electrical vehicles and wind turbines.

Kay Hameyer (M'96–SM'99) received the M.Sc. degree in electrical engineering from the University of Hannover, Hannover, Germany, in 1986 and the Ph.D. degree from University of Technology Berlin, Germany, in 1992, for working on permanent magnet excited machines.

After his university studies, he worked with the Robert Bosch GmbH in Stuttgart, Germany, as a Design Engineer for permanent magnet servo motors. From 1988 to 1993, he was a Member of staff at the University of Technology Berlin, Germany. From 1996 to 2004, he was a Full Professor of numerical field computations and electrical machines, Katholieke Universiteit Leuven (KU Leuven), Leuven, Belgium. Since 2004, he has been a Full Professor and the Director of the Institute of Electrical Machines, RWTH Aachen University, Aachen, Germany. His research interests include all aspects of the design, control and manufacturing of electrical machines and the associated numerical simulation. The characterization and modelling of hard- and soft-magnetic materials is another focus of his work. He has authored/coauthored more than 250 journal publications, more than 500 international conference publications and four books. His research interests include numerical field computation and optimization, the design and control of electrical machines, in particular, permanent-magnet excited machines, induction machines.

Dr. Hameyer has been a Member of the German VDE, since 2004 and a Fellow of the Institution of Engineering and Technology, U.K., since 2002.